When Firing Rate Falls Short: Spike Synchrony to Efficiently Disentangle Stimulus Saliency and Familiarity

Viktoria Zemliak[1,*], Pascal Nieters[1], Gordon Pipa[1,2]

[1]Institute of Cognitive Science, University of Osnabrück, Osnabrück, Germany

[2]Frankfurt Institute of Advanced Studies, Frankfurt, Germany

[*]Corresponding author: vzemliak@uos.de

Abstract

The function of temporal coding in the brain remains controversial, with debate centering on the following question: does spike timing information, such as their temporal synchrony, play a meaningful role in neural computation which cannot be attributed to firing rate? We propose the solution to this dilemma: spike synchrony provides crucial information about stimulus familiarity under conditions when the firing rate alone is insufficient − namely, when the input stimulus is varied in saliency. Using simulations of recurrent spiking networks, we show that synchrony is particularly effective in distinguishing familiar stimuli of low saliency from novel stimuli of high saliency − an important distinction for both biological perception and artificial agents navigating dynamic environments. We evaluate familiarity detection across two frameworks: a biologically inspired model of the primary visual cortex (V1) and an abstract associative memory model. We show that in both cases, synchrony is more sensitive to recurrent connectivity, that encodes prior experiences, compared to input firing rate. This highlights the relevance of synchrony for familiarity encoding in a scenario of realistic input variability.

Keywords: spiking networks; spike synchrony; temporal coding; familiarity detection; recurrent networks; associative memory.

Introduction

The concept of temporal coding in the brain has long been a subject of debate. It boils down to a single question: is firing frequency enough for neural computation, or does timing of spikes also play a crucial role (Softky & Koch, 1993; Shadlen & Movshon, 1999; Singer, 1999; Thorpe et al., 2001; Brette, 2015)? Spike timing can offer various mechanisms for encoding information, such as the precise order of spikes (Panzeri et al., 2014), latency to the first spike in response to a stimulus (Celebrini et al., 1993; Gollisch & Meister, 2010), synchronous firing across neurons, rhythmic oscillations at different frequencies (Buzsaki & Draguhn, 2004), bursting patterns (Naud & Sprekeler, 2018; Xie et al., 2024). Multiple studies highlight the question of reliability of spike timing, especially in the presence of noise (Mainen & Sejnowski, 1995; Ermentrout, Galán, & Urban, 2009).

In this context, spike synchrony as a form of temporal coding is highly debated. Researchers view it either as a mechanism binding input features into coherent representations (Roelfsema et al., 1996; Singer, 1999) or simply as a byproduct of firing activity (Shadlen & Movshon, 1999). Others propose that synchrony functions as a mechanism for coincidence detection (Abeles et al., 1991), working memory (Szatmáry & Izhikevich, 2010), invariant input coding (Brette, 2012), or relevant stimulus selection (Fries et al. 1997; 2002). A recent perspective suggests that synchrony in a recurrent network can act as a familiarity detector (Korndörfer et al., 2017; Zemliak et al., 2024; Zemliak et al., 2025), especially with well-separated strong connectivity clusters.

Familiarity is a simple form of recognition memory, which detects whether the stimulus has been encountered before. According to dual process theory, it is functionally and anatomically distinct from recollection, which extracts detailed information about the stimulus context from memory (Brown et al., 1987; Wolk et al., 2011; Scalici et al., 2017). Familiarity memory is essential for adaptive behavior in both living and artificial agents, enabling efficient decision-making based on prior experience. It can facilitate recollection of a well-known stimulus or, vice versa, the encoding of new stimuli in memory (Yonelinas et al., 1999; Yonelinas, 2001; Bülthof & Newell, 2006). Familiarity may be categorized by timescale into *absolute* and *relative* forms: absolute familiarity is linked to stable lifelong memories, while relative familiarity reflects recent exposure, e.g. on a timescale of a single experimental session. Relative familiarity is associated with repetition suppression along the visual processing hierarchy, from V2 to perirhinal cortex (PrC) (Xiang & Brown, 1998; Anderson et al., 2008; Huang et al., 2018), and is often modeled by feedforward and convolutional architectures with anti-Hebbian plasticity (Bogacz & Brown, 2003; Norman & O'Reilly, 2003; Kazanovich & Borisyuk, 2021; Tyulmankov et al., 2022). Interestingly, Huang et al. reported repetition enhancement in response to relative familiarity in V1 (2023). Absolute familiarity has been linked to increased activity in PrC, suggesting that well-consolidated, lifelong memory traces may engage distinct mechanisms (Duke et al., 2017; Yang et al., 2023). In this study, we focus on absolute familiarity footprints in a recurrent model.

Using simulations of recurrent spiking networks, we identify the conditions under which non-oscillatory, connectivity-driven synchrony carries crucial information which cannot be decoded from rate alone: it reliably detects absolute familiarity in stimuli of varied saliency. Rather than replacing rate coding, synchrony complements it: rate points to the relevant neuron population, i.e. encodes the stimulus content, and synchrony detects the stimulus' familiarity from the activity of its coding population. Moreover, once synchrony coding emerges in the

system, it can further take over the coding of the content of familiar stimuli too. We also explore different connectivity regimes and show that Rsync is resilient to drastic changes in the connectivity structure for familiarity detection. At the same time, connectivity structures, which are the most optimal for Rsync-based familiarity detection, lead to very energy-efficient network activity regimes.

Results

Stimulus meta-information

Stimulus saliency and familiarity are two kinds of meta-information about incoming stimuli. They don't convey information about the specific content of perceptions, such as which objects are depicted on an image, but rather provide a higher-level context about its relevance for processing and decision making.

Saliency. To define saliency in our study, we focus on bottom-up sensory characteristics of static stimuli, such as contrast and intensity, distinguishing saliency from relevance or priority, which involve top-down attention modulation (Fecteau & Munoz, 2006). Visual contrast and intensity influence firing rates across various brain areas, but we are most interested in thalamic firing rates as they provide feedforward input to visual processing regions (Rathbun et al., 2016; Sanchez et al., 2023), analogously to feedforward input in our simulations. Note that in many spiking models feedforward inputs are represented as Poisson processes with constant firing rates, disregarding meta-information about saliency. We argue that only in the context of variable stimulus saliency reflected in input firing rates, does spike synchrony exercise its computational potential, since it can reliably detect a different type of contextual information - input familiarity.

Familiarity. Familiarity memory was suggested to be encoded in recurrent (lateral) connections in computational models (Korndörfer et al., 2017; Zemliak et al., 2024). Consider an example of V1, where strong lateral connections are formed between neurons with similar receptive fields and in closer proximity to each other (Ts'o et al., 1986; Cossell et al., 2015), which aligns with Gestalt-like statistics of natural visual stimuli (for example, Sigman et al., 2001; Onat et al., 2013). Thus, recurrent connections in V1 reflect the acquired visual experience, and often experienced stimuli can be interpreted as familiar. At the same time, recurrent connection

strength also influences the level of spike synchrony (König et al., 1993; Stettler et al., 2002). Therefore, spike synchrony serves as a proxy to infer stimulus familiarity from firing activity (Korndörfer et al., 2017; Zemliak et al., 2024). Another prominent example of storing memory in recurrent connections is the hippocampal region CA3. Its pyramidal neurons form ensembles of recurrent connections which strengthen with experience and participate in associative memory recall (Nakazawa et al., 2002). Then, synchrony can be used to decode familiarity signals from the neural activity shaped by such recurrent connectivity.

Every input stimulus can be characterized in terms of meta-information about its saliency and familiarity, in addition to the actual stimulus content. If we simplify both features to binary classes (familiar vs novel, salient vs weak), all stimuli can be categorized into 4 groups: A. familiar and salient; B. new and salient, C. familiar and weak; D. new and weak (see Fig 1).

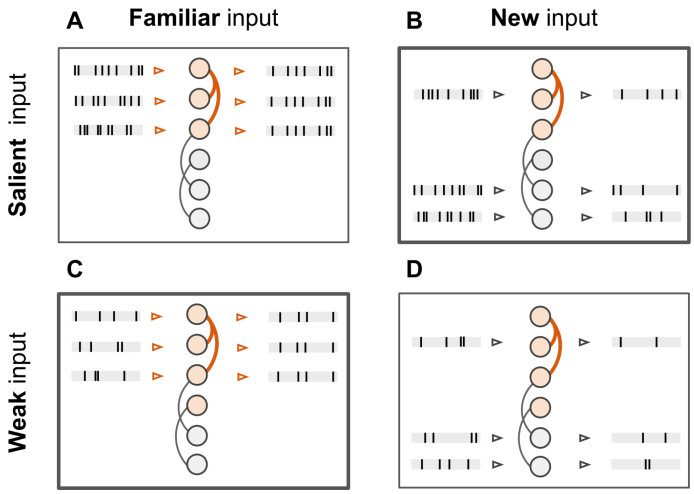

Fig 1. The impact of input saliency and familiarity

Input stimuli can be divided into 4 groups based on their meta-information: **A**. Familiar and salient, **B**. New and salient, **C**. Familiar but not salient (weak), **D**. New and not salient. Saliency is represented by the input firing rate, and familiarity by strength of recurrent connectivity. When saliency varies, output firing rate (spike count) can be similar between conditions B and C. They can only be reliably distinguished by spike synchrony.

Unlike output firing rate, synchrony can distinguish between two crucial types of sensory inputs: B and C, i.e. between the feedforward and recurrent input sources. Such distinction is important for efficient functioning in dynamic environments, e.g. recognizing a barely visible yet familiar dangerous stimulus versus an unfamiliar but salient one. For artificial agents, it is equally important to identify previously encountered objects or situations while reacting appropriately to new inputs.

Experiments

We tested two 1000-neurons recurrent spiking models for input familiarity detection: (i) a network with a V1-like connectivity structure and (ii) an abstract associative memory model. The first model is biologically grounded and provides insights into the familiarity readout mechanism in the primary visual cortex (see Methods V1 model connectivity). In contrast, the second, more abstract model allows for systematic manipulation of recurrent connectivity parameters, including the size and quantity of familiar input representations and the structure of inhibition.

For each sample in our simulations, the external input was delivered to a subset of neurons (weakly interconnected for new, and strongly interconnected for familiar) via one-to-one connections in a form of asynchronous uncorrelated Poisson spike trains at the same constant rate for that sample. The input rate of each data sample was drawn from a uniform range of possible input firing rates. For the V1 model, we tested different input rate ranges, and for the abstract model all experiments were performed for the range of 10-90 Hz. Thus, in both experiments we varied the saliency (rate) of inputs across data samples, for new and familiar stimuli alike.

A single dataset included 320 data samples: 160 familiar and 160 new stimuli. For the V1 model, the familiar stimuli were clusters of 40 neurons with a similar spatial and orientation selectivity, and for the abstract model the familiar inputs were pre-generated groups of 100 neurons which were embedded as strongly connected clusters into the connectivity structure. New inputs in both models were randomly chosen groups of neurons, similar size as familiar stimuli. The dataset structure can be seen in Fig 2A.

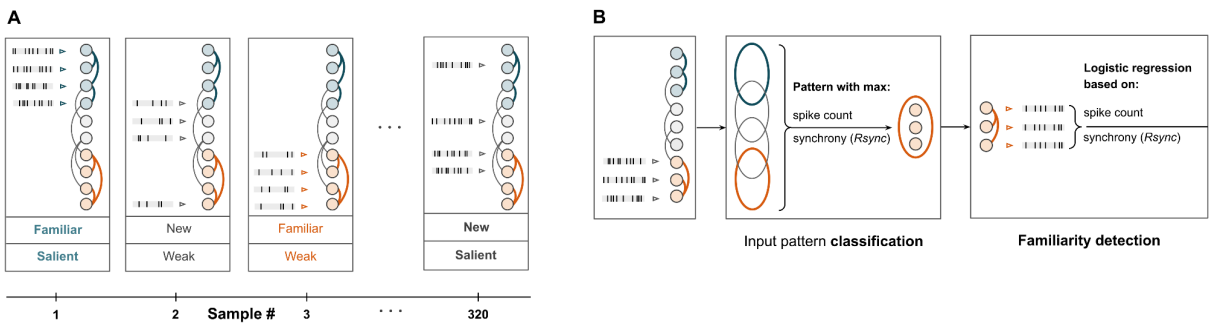

Fig 2. Dataset & experimental pipeline for familiarity detection

Teal and orange colors represent strongly connected clusters, i.e. familiar memories. **A**. Dataset for both experiments (V1 and associative memory model): 160 new and 160 familiar stimuli in random order, with varied saliency (input rate). **B**. The abstract model of associative memory encodes multiple familiar stimuli. It first has to identify which neurons receive the feedforward input and then use this group of neurons to detect pattern familiarity.

We tested multiple experimental conditions in our simulations. For the V1 model, we tested different scales of input saliency variability: 0 (fixed input firing rate 50 Hz), 10 (40-60 Hz), 20 (30-70 Hz), 30 (20-80 Hz), 40 Hz (10-90 Hz), and for the abstract model the number of pre-encoded patterns: 100, 200, 300, 400, 500. For every condition, we performed 20 iterations with a full dataset each, and measured average performance in familiarity classification.

To predict whether a sample was new or familiar, we used the model's firing activity in response to the sample stimulus. We employed univariate logistic regression for binary classification (1 = familiar, 0 = new), using either firing rate or spike synchrony statistics as predictors. Firing rate was computed as average spike count (SC), and spike synchrony was computed as Rsync:

$$SC(P,T) = \frac{1}{P}\sum_{i=1}^{P} SC_i(T) \tag{1}$$

$$R_{sync}(P,T) = \frac{\widehat{Var}\left[\langle A_i(t)\rangle_{i\in P}\right]_{t\in T}}{\left\langle \widehat{Var}\left[A_i(t)\right]_{t\in T}\right\rangle_{i\in P}} \tag{2}$$

Here, P defines the externally-stimulated neuron population representing one encoded pattern, and $T = 500$ ms is a time interval for measuring spike count or synchrony. Eq. 1 describes

population spike count SC, which is measured as an average spike count of all neurons in the population representing one pattern.

In Eq. 2, Rsync measures spike synchrony by comparing the variance of the population mean activity to the average variance of individual neurons. A_i is an activation trace of neuron i from neural population P. To compute activation traces, raw binary spike trains were first convolved with an exponential kernel $k(t) = \exp(-t/\tau)$, with timescale $\tau = 5$ ms. If all neurons fire in perfect synchrony, their activity traces are identical, so the variance of the mean field equals that of individual neurons, yielding $Rsync = 1$. Likewise, if neurons fire independently, the mean field gets averaged out and flattened, and $Rsync \to 0$. Unlike pairwise correlations, $Rsync$ is a group measure which scales to populations of any size.

For each model, we defined network connectivity structure, selected neurons for performance measurements and reported F1 scores obtained through 10-fold cross-validation. We also show baseline scores for random predictions.

Synchrony detects familiarity under increasing input variability in V1 network

In the first experiment, connectivity models the structure of horizontal connections in V1, with connections and weight distribution based on experimental observations (see Methods V1 model connectivity). Familiar input patterns in the network were represented by clusters of 40 spatially neighboring neurons with similarly tuned receptive fields and strong mutual connectivity. Such pattern structure reflects the core principle of Hebbian plasticity in V1: neurons that are frequently co-activated tend to develop stronger synaptic connections over time and thus reflect the acquired visual experience (Galuske & Singer, 1996; Schmidt et al., 1999). We assume that the prior experience with repeatedly occurring visual patterns leads to the emergence of tightly connected neuronal clusters. We refer to such experience as familiarity, and hence these clusters represent familiar patterns in our model. The pattern size of 40 is consistent with the cluster analysis of neurons in L2/3 of V1 (Baker & Gong, 2023; Carrillo-Reid, 2019).

Input familiarity detection. We examined how familiarity detection performance depends on the subset of neurons used for measuring predictor features. Specifically, we compared classification accuracy when spike synchrony or average firing rate were measured in: (a) all neurons in the

model, (b) the subset of neurons receiving external feedforward input (Fig 3A). Both spike synchrony and spike count perform better when evaluated for a group of neurons receiving the feedforward stimulus input rather than for an entire network, but for spike count the difference is less pronounced.

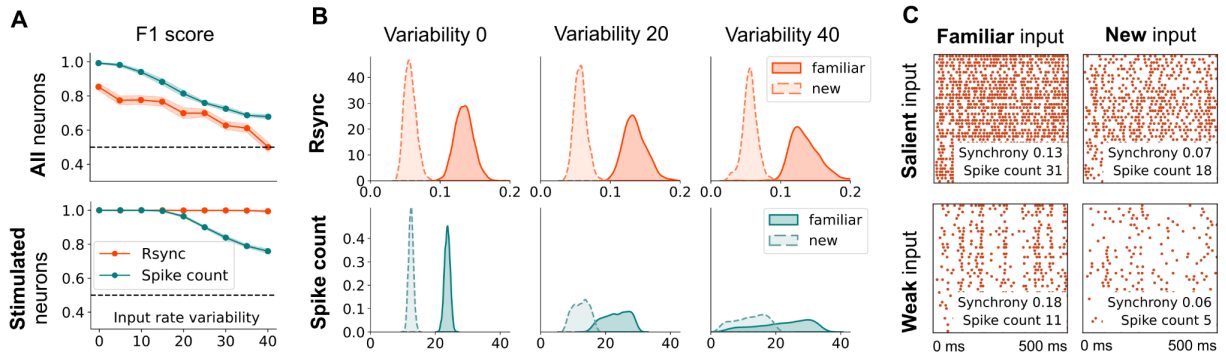

Fig 3. Familiarity detection for V1 model for different saliency (input rate) variability

Cross-validated performance of Rsync- and spike count-based classifiers for detecting input familiarity from all neuron activity and from the activity of externally stimulated neurons, averaged over 20 trials. Every trial includes 360 data samples, input saliency (firing rate) variability changed from 0 (50 Hz) to 40 (10-90 Hz). Rsync outperforms spike count for higher rate variability. **A**. Averaged F1 score for different input saliency (firing rate) variability. **B**. KDE plots of synchrony and spike count of stimulated neurons in response to new and familiar stimuli. **C**. Example spike raster plots of 500 ms of network activity in response to weak (10 Hz input rate) and salient (90 Hz input rate), new and familiar stimuli, with spike synchrony and average population spike count for every condition.

At the same time, synchrony works better as a localized measure. Note that local synchrony-based familiarity classification performance remains very robust under the conditions of saliency (input rate) variability, which reveals its particular sensitivity to input familiarity.

Distributions of spike count and synchrony. We examined the distributions of spike synchrony and spike count among stimulated neurons (Fig 4B). Spike synchrony distributions remained well-separated across all input variability conditions, while spike count distributions became indistinguishable under higher input variability. This demonstrates that spike synchrony

can be a reliable indicator of familiarity in dynamic environments: firing activity becomes more temporally coherent upon encountering a familiar stimulus (Fig 4C).

Synchrony detects familiarity under high memory load

To investigate the computational potential of recurrent connectivity in familiarity detection, we conducted a similar experiment in an abstracted SNN model, free from V1-specific receptive fields and connectivity constraints shaped by real-world visual statistics. The model included 5000 neurons. We increased the size and number of tightly connected clusters to examine the network's memory capacity, but maintained a log-normal weight distribution for consistency and biological realism.

Familiar patterns & connectivity. We generated n random binary patterns of size 100 to represent familiar stimuli, which we encoded in the network connectivity. For each pattern, every neuron activated by that pattern sent excitatory projections to other neurons in the same pattern with probability 0.4. The quick emergence of such clusters and their use for familiarity recognition has been demonstrated in rate (Tyulmankov et al., 2022), excitatory spiking (Zemliak et al., 2025), and balanced E-I (Litwin-Kumar & Doiron, 2014) networks. These clusters naturally emerge via Hebbian learning when groups of neurons are co-activated by perceived stimuli. We omitted simulation of this plasticity process in our model and simply inferred the resulting connectivity. Additionally, we implemented cross-pattern inhibition by connecting neurons to neurons outside their pattern with probability 0.04. Thus, each neuron was allowed to form outcoming excitatory connections within its cluster and inhibitory connections with neurons from the other clusters, with given probabilities. This approach is well-established in associative memory models and can be seen as a spiking implementation of negative connections in Hopfield networks (Hopfield, 1982). In the brain, heterosynaptic inhibition is hypothesized to be crucial for pattern distinction in higher-order processing areas such as the hippocampus (Koolschijn et al., 2019; Lovett-Barron et al., 2014). All weights in our model were independently drawn from a log-normal distribution.

Experimental setup. All experiments were conducted in the most challenging input setup in which the variability of the input rate was set to maximal 40 Hz emulating high variability in stimulus salience. We repeated the following experimental procedure 20 times: we first encoded 100 to 500 randomly-generated familiar patterns in recurrent connectivity resulting in a network model. From these encoded familiar patterns, we then created a dataset of 160 familiar

patterns, added 160 new patterns and then recorded the network activity in response to this 320 patterns dataset. We then attempted to classify their familiarity using SC or Rsync values. Based on the performance in V1 experiments, these values were measured within the externally stimulated neurons. This decision motivated us to address an additional computational challenge (see Fig 2B):

1) First, the network had to identify the subset of neurons receiving the external input. This was achieved by selecting an input pattern with the highest spike count or synchrony out of all pre-encoded familiar patterns + new patterns. We evaluated the results of pattern identification as a multiclass classification, using F1 scores equally weighted across classes (Fig 5). Spike count demonstrated superior results in terms of identifying an externally stimulated pattern. Thus, we used spike count-based pattern identification, to further predict the familiarity of the identified pattern.

2) SC and Rsync were computed for patterns identified in each of 320 trials. Then, we trained a binary logistic regression classifier on these 320 data samples to predict the pattern familiarity, based either on Rsync or SC values used as features. The performance was evaluated as an average F1-score in a 10-fold cross-validation procedure. (Fig 4).

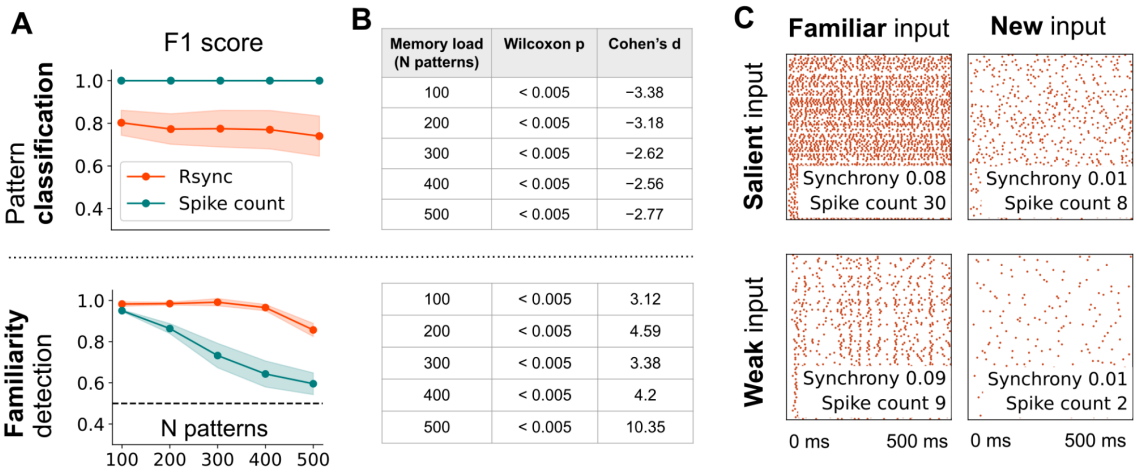

Memory load (N patterns)	Wilcoxon p	Cohen's d
100	< 0.005	−3.38
200	< 0.005	−3.18
300	< 0.005	−2.62
400	< 0.005	−2.56
500	< 0.005	−2.77

100	< 0.005	3.12
200	< 0.005	4.59
300	< 0.005	3.38
400	< 0.005	4.2
500	< 0.005	10.35

Fig 4. Familiarity detection and pattern classification for the associative memory model

Cross-validated performance of Rsync- and spike count-based classifiers for detecting a stimulated group of neurons and the familiarity of a pattern which they are encoding, averaged over 20 trials. Every trial includes 360 data samples, input saliency (firing rate) variability across samples 40 Hz. For all amounts of pre-encoded patterns, Rsync outperforms spike count in familiarity detection, but falls behind in input classification. **A**. Averaged F1 score for different amounts of pre-encoded patterns. **B**. Wilcoxon test for

significant differences between Rsync and spike count and Cohen's d for the effect size. **C**. Spike raster plots of 500 ms of network activity in response to weak (10 Hz input rate) and salient (90 Hz input rate), new and familiar stimuli, with synchrony and average population spike count.

Nearly all stimulated patterns were detected with 100% accuracy using average spike count, enabling familiarity detection from identified neurons. The Wilcoxon test showed significant superiority of spike count over Rsync for the identification of a stimulated pattern (Fig 5B). In contrast to classification, spike synchrony performed significantly better in a familiarity detection task under the maximum input saliency (input rate) variability 40 Hz (input rate range 10-90 Hz). The effect size measured as Cohen's d was the strongest for the most challenging experiment condition: 500 pre-encoded familiar patterns (Fig 4B). However, Rsync has an important limitation in terms of familiarity classification: it strongly relies on accurate pattern classification. Spike count and spike synchrony thus provide complementary information about the stimulus — its content and familiarity, respectively.

Both familiarity detection metrics show declining performance as the number of familiar patterns stored in the network increases. This effect aligns with Zemliak et al. (2025), who attribute it to growing overlap between clusters representing familiar patterns. In the next section, we show how this effect can be counteracted by regulating the proportion of excitatory and inhibitory connections.

Rate and synchrony encode complementary information across various connectivity structures

To ensure that the superior performance of spike synchrony in familiarity detection was not due to a specific parameter setting, we systematically explored the parameter space defined by the proportions of excitatory and inhibitory connections. We compared the performance of rate-based and synchrony-based familiarity classification across a broad range of connectivity regimes, and also assessed how these same networks performed on two related tasks: pattern classification and pattern completion. Due to the computational demands of testing all parameter combinations, we conducted these experiments on reduced networks of 1000 neurons, using weight amplitudes and distributions consistent with previous simulations.

The parameter space was defined by two variables: the proportion of log-normally distributed excitatory connections within each pattern, and the proportion of log-normally distributed cross-pattern inhibitory connections. Across all parameter settings, we kept all other parameters fixed, varying only the sparseness of excitatory and inhibitory connections. This allowed for a controlled comparison of network performance across different connectivity regimes (Fig 5).

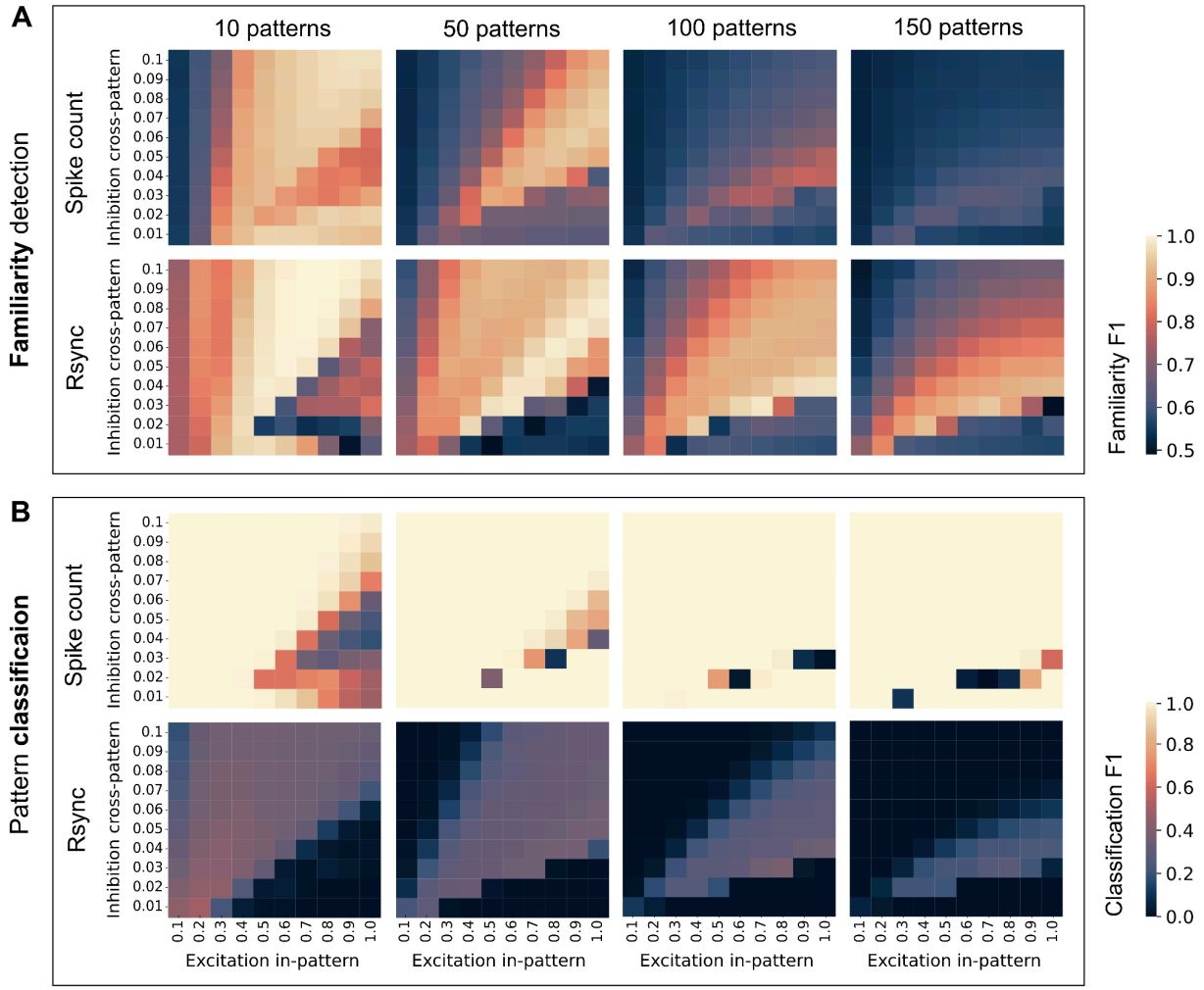

Fig 5. Familiarity detection and pattern classification across connectivity parameters

Cross-validated performance of Rsync- and spike count-based classifiers, for every combination of the proportion of in-pattern excitatory connections and cross-pattern inhibitory connections. Averaged over 10 trials, every trial includes 360 data samples, input saliency (firing rate) variability across samples 40 Hz. Spike count performs better at pattern classification, while synchrony excels at familiarity detection,

especially for more encoded patterns. **A**. F1-score in familiarity detection. **B**. Macro F1-score in pattern classification.

Familiarity detection. Rsync outperformed spike count in familiarity classification across all tested parameter combinations and exhibited consistently high performance across a broader range of connectivity regimes (Fig 6A). In other words, Rsync was more robust to variations in network connectivity. This robustness is important, as connectivity can vary due to plasticity-driven changes in how inputs are encoded in the excitatory population, and due to changes in the level of competition between patterns, which is modulated by the density of inhibitory connections. As such, Rsync appears as a reliable familiarity detection metric, even when the precise connectivity structure is variable or uncertain. In contrast, spike count-based familiarity detection was only reliable in networks with a low number of encoded patterns − conditions that correspond to minimal pattern overlap. Even in this limited regime, spike count was more sensitive to the balance between excitatory and inhibitory connections, making it less reliable when connectivity is dynamic or noisy.

Both Rsync and spike count perform best in networks with a balanced connectivity profile, where the total excitatory input to a neuron (i.e., the sum of recurrent excitatory weights) is equal or slightly less than the total inhibitory input, which can be achieved through approximately 3:2 ratio of excitatory to inhibitory incoming connections (see Supplementary Fig S1). For instance, in a 1000-neuron network where each pattern activates 100 neurons, an excitatory sparseness of 0.8 corresponds to 80 recurrent excitatory connections per neuron, while an inhibitory sparseness of 0.06 corresponds to 54 inhibitory connections. At higher memory loads (with more encoded patterns), optimal connectivity shifts toward increased excitation and reduced inhibition. This adjustment compensates for greater between-pattern overlap, which increases the likelihood that non-target patterns become partially activated by external input. Such cross-activation amplifies inhibitory competition, and to ensure stable activation of the correct pattern, sufficient excitation is required to overcome this excess inhibition. A more efficient connectivity structure might be achieved by concentrating excitatory connections between neurons representing minimally overlapping patterns, potentially through ongoing plasticity. However, the design of such plasticity mechanisms are beyond the scope of the present work.

Pattern classification. In contrast to its role in familiarity detection, spike count outperforms Rsync in classifying incoming patterns, regardless of the network's connectivity structure (Fig

5B). Rsync is less reliable in detecting new patterns, particularly when they overlap with familiar ones. This is because familiar patterns tend to evoke strong synchronous firing, reflecting the presence of established recurrent connections. New patterns, by contrast, typically have weaker within-pattern connectivity, leading to lower levels of recurrent input. Since Rsync relies more heavily on recurrent dynamics than on feedforward input, its ability to distinguish between new patterns is limited. Spike count, however, is more directly influenced by feedforward drive, making it better suited to identifying which specific pattern is currently active. In summary, spike count more effectively decodes the identity of the input, while Rsync provides a stronger signal of how well the input matches the network's learned connectivity.

The complementary roles of spike count and synchrony are further supported by a control analysis (see Supplementary Fig S2), in which familiarity detection was performed using activity measurements from the entire network rather than from the classified pattern exclusively. Under this global decoding scheme, Rsync-based familiarity detection performance declined as the number of stored patterns increased. This result underscores the limitations of synchrony and highlights the benefit of combining it with spike count for robust decoding. In summary, successful execution of both tasks − familiarity detection and pattern classification − depends on a specific balance of excitatory and inhibitory input to each neuron. This balance is attainable through a limited subset of connectivity configurations, regardless of whether familiarity is decoded via spike count or synchrony. Among these configurations, spike synchrony favors regimes characterized by lower overall activity (Fig 6).

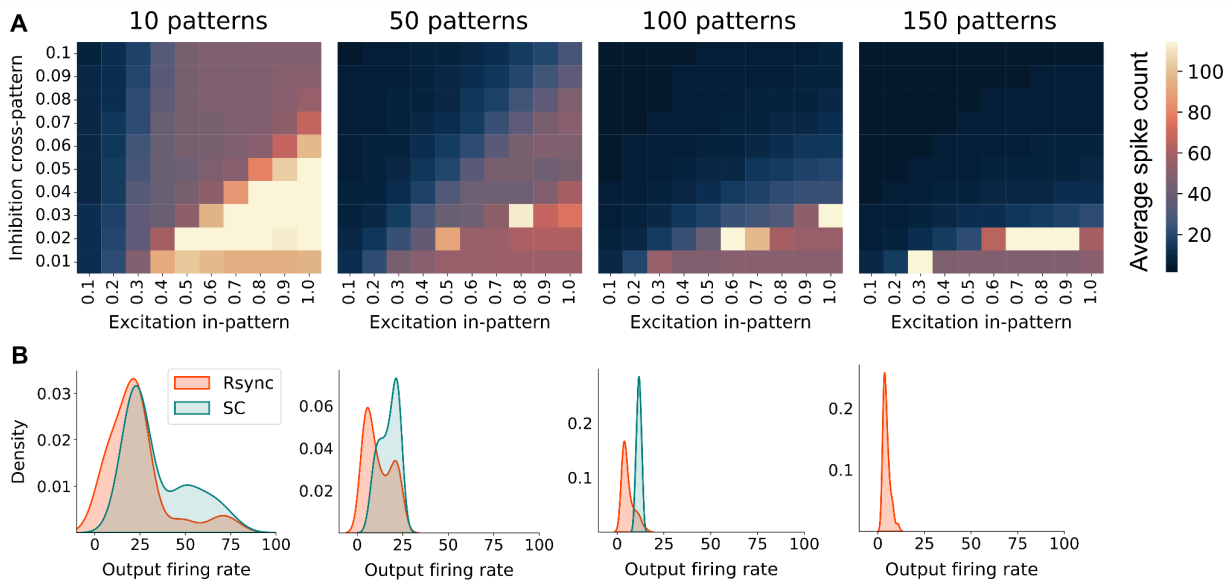

Fig 6. Network activity across connectivity parameters

Network activity is measured as the average output firing rate, for combinations of the proportion of in-pattern excitatory connections and cross-pattern inhibitory connections, with input saliency (firing rate) variability across samples 40 Hz. **A**. Average output firing rate. **B**. Macro F1-score in pattern classification. **C**. Distribution of output rate for parameter combinations that lead to F1 > 0.75 on a familiarity detection task. For 150 patterns, there is no parameter regime which would lead to this performance in a spike count familiarity detector. For networks with 10, 50, and 100 neurons, the distribution of Rsync values is significantly lower than that of spike count values (Mann-Whitney U test, $p < 0.005$ for all comparisons).

Parameter combinations optimized for familiarity detection using Rsync, and result in significantly lower overall network activity compared to those optimized for spike count-based detection, regardless of the number of presented patterns. This suggests that spike synchrony offers a more efficient mechanism for decoding familiarity under conditions of variable input saliency. It operates effectively across a wider range of parameter regimes and does so with greater accuracy and energy efficiency. At the same time, spike count more reliably captures complementary information about stimulus content. Together, the two metrics provide a more robust decoding of stimulus properties than either alone.

From rate to synchrony coding

Our experiments showed that, in recurrent spiking systems, familiarity decoding of inputs with varied saliency relies on synchrony-based representations. In contrast, pattern classification is primarily supported by rate coding. Thus, stimulus content is propagated via firing rate, whereas spike synchrony conveys familiarity meta-information. This raises a natural question: once synchrony emerges through recurrent activity in response to familiar inputs, does their coding scheme change as they ascend the sensory processing hierarchy? Here, we hypothesized that not only does synchrony arise as a result of recurrent processing in the initially rate-coded system, but once established, it can serve as a more effective input code for the downstream propagation of familiar stimuli. To test this hypothesis, we performed both familiarity detection and pattern classification based on the activity evoked by temporally synchronous − rather than Poisson − input, assuming that this input was synchronized in a preceding area. The level of input synchronization was also measured as Rsync, with Poisson patterns yielding input Rsync 0.0. We tested input Rsync levels 0.1, 0.2, 0.6, 1.0 (Fig 7; see also Methods Synchronized input generation).

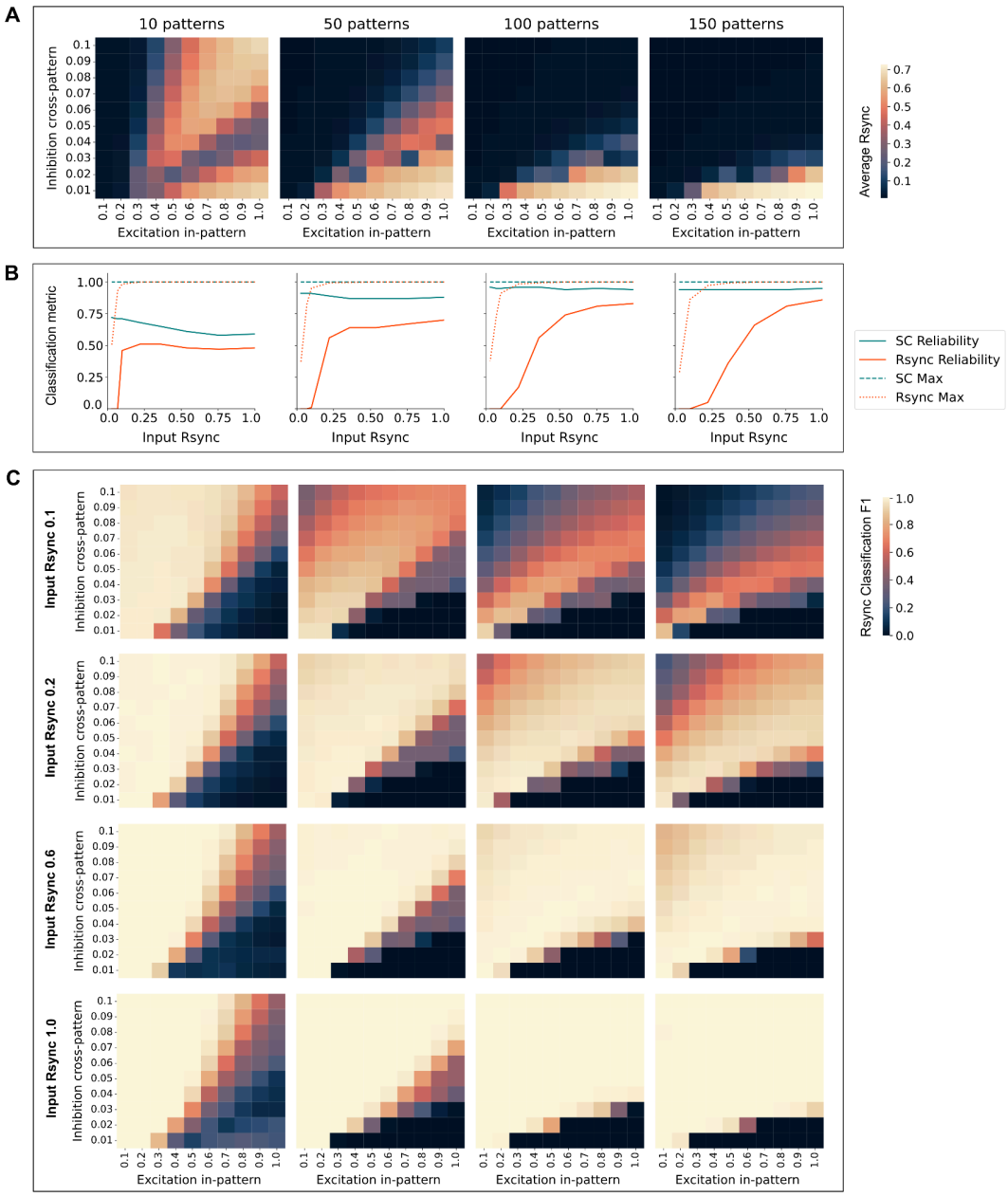

Fig 7. Rsync for synchronized inputs classification

A. Average Rsync values Poisson inputs range from 0.08 to 0.75. **B**. Rsync and SC (spike count) reliability (the number of parameter configurations yielding F1 > 0.95) and maximal performance (maximum F1 across the configurations) for classification of patterns of different synchrony: 0.1, 0.2, 0.6, 1.0. Averaged over 10 trials, every trial includes 360 data samples, input saliency (firing rate) variability across samples 40 Hz. The more synchronized the inputs are, the more reliably Rsync can be used to classify them. **C**. F1 on Rsync-based pattern classification across the parameter configurations for input synchronization values: 0.1, 0.2, 0.6, 1.0.

Temporal synchronization of input patterns did not significantly affect familiarity detection performance: Rsync consistently outperformed spike count across a wide range of parameter configurations (see Supplementary Fig S3). Similarly, spike count-based classification of pattern identity remained stable regardless of the degree of input synchrony (see Supplementary Fig S4). In contrast, Rsync-based pattern classification was sensitive to input synchronization: it failed to classify fully decoherent Poisson inputs (see Fig 5), but performance improved with increasing synchrony (Fig 7B-C). Under low memory loads − i.e., when fewer than 150 patterns were stored − Rsync reliably achieved high classification accuracy even with modest input synchrony. When inputs were perfectly synchronized, Rsync maintained high accuracy across nearly all parameter configurations, making it a highly reliable pattern classifier, almost as reliable as spike count-based classification. These findings suggest that once neural activity becomes synchronized at a particular processing stage, this temporal coherence can propagate through the sensory hierarchy, allowing both stimulus identity and familiarity to be decoded from spike synchrony alone.

Synchrony appears to be an especially effective code for familiar patterns. When a pattern has been encountered before and induced Hebbian plasticity, strengthened recurrent connections lead to more synchronized responses, which Rsync can classify reliably. This synchrony can propagate through subsequent layers, allowing both identity and familiarity to be decoded from the temporal structure of spike trains. In contrast, new patterns − activating neurons with weaker recurrent connectivity − produce more asynchronous responses, making spike count a more reliable signal. Thus, the network can encode familiar stimuli primarily through synchrony, while falling back on rate coding for novel inputs that have not yet shaped strong recurrent representations.

Discussion

In this study, we have shown that synchrony in a recurrent spiking neural network outperforms spike count as a measure of stimulus familiarity when input salience (modeled as varied input firing rate) changes. Input familiarity detection is vital for both artificial agents and living organisms, helping identify environmental changes and enabling adaptation. Reliable familiarity decoding under varied conditions allows quick detection of known dangerous or rewarding stimuli. From the perspective of Bayesian models and the predictive coding framework, familiar inputs match prior expectations, while new inputs require prediction updates. Computationally, synchrony-based familiarity decoding can support completion and retrieval of familiar patterns

encoded as interconnected neuronal clusters, potentially determining which engram can be or has been completed based on synchrony scores. Many studies have explored phase-coded patterns as associative memory (e.g., Scarpetta & Giacco, 2012; Frady & Sommer, 2019), with empirical evidence supporting phase synchrony's role in memory formation (Clouter, Shapiro, & Hanslmayr, 2017; Palva, Palva, & Kaila, 2005; Sweeney-Reed et al., 2014). Future research should explore how non-oscillatory Rsync supports memory completion and retrieval.

In our model, stimulus familiarity is represented by its match to existing recurrent connectivity, while saliency is defined by the input firing rate. It was already shown that recurrent connectivity can store information about prior experiences in strongly connected clusters (Litwin-Kumar & Doiron, 2014; Korndörfer et al., 2017; Zemliak et al., 2024). They are shaped by Hebbian plasticity in various network architectures upon the exposure to external stimuli (Hopfield, 1982; Litwin-Kumar & Doiron, 2014; Tyulmankov et al., 2022, Zemliak et al., 2025). To our knowledge, this study first compares rate and temporal strategies for retrieving familiarity information under varied input saliency. Our results show that spike synchrony responds more to recurrent connections than input rate, while output rate fails to separate these contributions. Our findings seem to contradict previous work of our group (Zemliak et al., 2025), where we found spike count outperforms synchrony for familiarity detection in recurrent networks. However, the aforementioned study used Poisson input with constant firing rates, while we show synchrony's advantage emerges with varying input rates that better reflect real-world visual input. This extends Brette's (2012) theory of synchrony as a mechanism for invariant coding. By testing input saliency variation specifically, we demonstrate how it disrupts spike count-based familiarity decoding while synchrony remains robust.

Our results show that spike synchrony is most effective as a localized phenomenon, particularly when measured in the subset of neurons receiving strong feedforward external input, and identifying this specific group of neurons requires incorporating spike count into the analysis, , as synchrony alone cannot reliably detect the neural population corresponding to unfamiliar patterns. This limitation arises from synchrony’s dependence on recurrent connectivity: novel inputs engage weakly connected clusters, which fail to generate the synchronous activity necessary for classification. Conversely, familiar patterns that partially overlap with novel inputs may produce spurious synchrony, leading to false-positive classifications. These findings suggest that spike synchrony and spike count provide complementary information about incoming stimuli, when they are encoded as noisy Poisson spike trains. Spike count more

reliably identifies the input pattern, while spike synchrony conveys meta-information about the match between the input and the network's recurrent structure.

However, when strong synchrony is imposed on the input patterns instead of using Poisson spike trains, output synchrony successfully serves both as a familiarity detector and as a reliable pattern classifier. In this case, even weakly connected (novel) clusters behave like strong ones − not by engaging recurrent attractors, as familiar inputs do, but by achieving reliable activation through precise spike timing in the input. Thus, once activity synchronizes at a certain processing level, all information about the stimulus can be further propagated via synchrony coding. This result is consistent with anatomical and functional connectivity in the visual processing system in the brain. The activity of LGN − an early sensory processing area − is predominantly driven by vertical (feedforward or feedback) connections and lacks lateral excitatory inputs (Derrington, 2001), which favours rate-based representations. Then, higher cortical areas exhibit dense recurrent connectivity: from primarily like-to-like excitatory horizontal connectivity in V1 (Cossel et al., 2015; Lee et al., 2016), though broader contextual interactions have also been reported (Chavane et al., 2011 and Huang et al., 2014), to less selective connections in V2 (Malach et al., 1994; Levitt et al., 1997) and highly diverse connectivity between columns with different selectivity in IT (Tsunoda et al., 2001; Hu et al., 2025). This anatomical gradient supports an idea of a functional transformation: from purely rate-coded inputs to representations in higher-order areas where synchrony plays an increasingly functional role, naturally emerging from strong recurrent connectivity.

Our V1 model behaves differently from empirical findings reported across multiple cortical areas, including V2, the inferotemporal cortex (IT), and the prefrontal cortex, where repetition suppression is commonly observed (Brown et al., 1987; Rainer & Miller, 2000; Anderson et al., 2008). However, some studies also report an initial enhancement of neural responses to familiar stimuli before suppression occurs. For instance, Rathbun et al. (2016) demonstrated that phase-reversing familiar visual stimuli in V1 elicit an initial increase in firing rate, followed by prolonged suppression, suggesting that familiarity-induced excitation triggers strong inhibition. However, our implementation of inhibition is relatively simplistic, lacking explicit modeling of dynamic interactions between excitatory and inhibitory neurons. Future work could explore a more detailed representation of multiple neuronal classes.

We also analysed connectivity parameter spaces optimal for familiarity detection and pattern classification. Both tasks lead to high performance across a broad range of connectivity

configurations. Spike count-based classification is particularly robust, with nearly perfect performance across almost the entire parameter space. Familiarity detection is also robust when detected from spike synchrony, but becomes more sensitive at higher pattern loads, suggesting a greater reliance on inhibitory control to prevent interference. The optimal parameter regimes for synchrony-based familiarity detection evoke less overall firing activity. Thus, temporal coding of stimulus familiarity enables a recurrent spiking network to function in a more energy-efficient regime. These results suggest that synchrony is a more scalable code for familiarity detection under biologically realistic constraints such as limited resources and high memory interference.

To conclude, our results highlight spike synchrony as a powerful mechanism for input familiarity detection, as it indirectly reflects the structure of recurrent connectivity while remaining robust to fluctuations in input firing rate. This underscores the potential of synchrony-based familiarity decoding in real-world scenarios involving dynamic visual stimuli. Ultimately, we believe that a combination of temporal and frequency-based characteristics of neural activity is necessary for recurrent spiking systems to interact effectively with changing environments.

Methods

Spiking model

In our experiments, we used spiking recurrent networks (SNNs) composed of 5000 Leaky Integrate-and-Fire (LIF) neurons. The membrane potential of neurons evolves according to the equation

$$\tau_m \frac{dV_i}{dt} = -(V_i - E_L) + RI_i(t) \tag{3}$$

Here, dV is an update of membrane potential per timestep $dt = 1.0$ ms, resting potential $E_L = -65$ mV, membrane time constant $\tau = 10$ ms. The firing threshold in the model is set to -55 mV, and the refractory period equals 3 ms. $I_i(t)$ are the synaptic currents arriving at the soma:

$$RI_i(t) = \tau_m \left(I_i^f(t) + I_i^E(t) + I_i^I(t) + \eta_i(t) \right) \tag{4}$$

$$I_i^E(t) = \sum_j w_{ij}^E S_j^E(t), I_i^I(t) = \sum_j w_{ij}^I S_j^I(t) \tag{5}$$

$$I_i^f(t) = \sum_j w^f S_j^f(t) \tag{6}$$

These currents include summed input from feedforward, recurrent excitatory and recurrent connections, scaled by corresponding PSP efficacy values w^f, w_{ij}^E and w_{ij}^I. $S_j(t)$ denotes a presynaptic spike arrival as the Dirac delta function $S_j(t) = \delta(t - t_j)$. All feedforward weights are equal and set to 3. We did not simulate separate excitatory and inhibitory neuron populations. Instead, each neuron projects both excitatory and inhibitory outputs, defined by two distinct recurrent connectivity matrices. External input is delivered via one-to-one feedforward connections, modeled as a Poisson process.

Additionally, we model random fluctuations of the membrane potential due to stimulus independent background activity by including the Gaussian white noise term $\langle \eta_i(t) \rangle = 0.5$ and $\sigma^2 = 0.5$ mV. The membrane noise is uncorrelated across neurons and time and biases neurons towards firing so that they can be driven effectively by very sparse Poisson inputs within our 500 ms simulation time. We chose maximal $\langle \eta_i(t) \rangle$ and σ^2 values under which neurons only fire upon receiving external input, despite the noise. Thus, neurons' membrane potentials were consistently kept in a subthreshold state.

V1 model connectivity

Each neuron in the model has a receptive field defined by spatial and orientation selectivity. The model is designed to recognize 8 orientation angles (from 0° to 180° in 22.5° steps) using 800 neurons, each tuned to a specific orientation. These neurons are arranged in a 10×10 grid representing a visual field. We measure distance between neurons as Chebyshev distance − the maximum difference along any coordinate dimension, appropriate for a 2D grid setup. Each unit of difference corresponds to 100 μm.

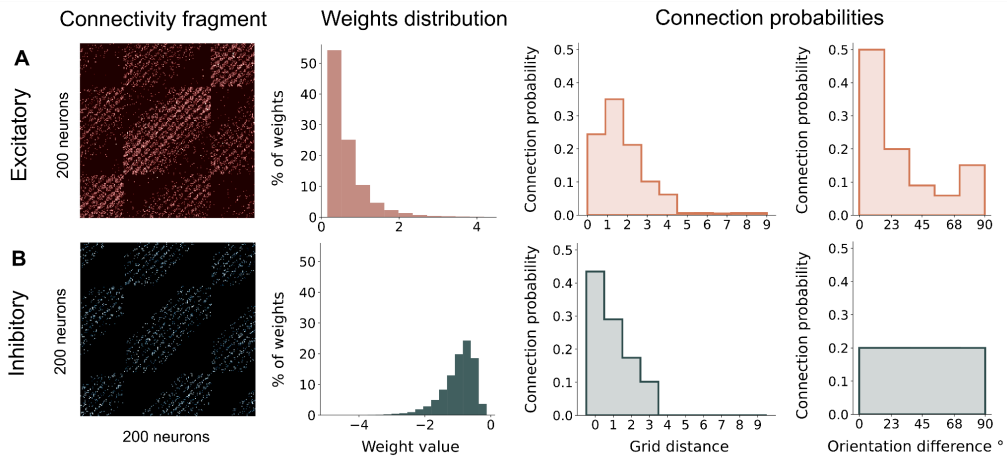

Fig 8: An example of V1 model connectivity. A fragment (200 neurons) of a heatmap, connection weights distribution, connection probabilities of the excitatory connectivity matrix of the: **A**. excitatory connectivity matrix, **B**. inhibitory connectivity matrix.

Excitatory connections exhibit 10% sparseness and follow a log-normal weight distribution, consistent with measurements of pyramidal neuron connectivity in layers 2/3 of V1 (Cossel et al., 2015; Hage et al., 2022). Connection probability depends on both spatial proximity and receptive field similarity. While most connections form over short distances, the model also includes a small number of strong long-range recurrent connections, in line with empirical observations (Bosking et al., 1997).

Inhibitory connections are modeled after Parvalbumin expressing (PV) interneurons − the prevalent type of inhibitory interneurons in layers 2/3 of V1. These neurons exhibit weak orientation selectivity (Niell & Stryker, 2008), in our model simplified to no orientation selectivity, as in Taylor et al. (2024). The inhibitory connectivity depends on distance, follows log-normal distribution (Hage et al., 2022; Znamenskiy et al., 2018) and has a total sparseness of 6% (20% within 300 μm). As a result, our V1 model has a broad, non-selective inhibitory mechanism that serves primarily to regulate overall excitatory activity, which could otherwise destabilize the recurrent network.

Synchronized input generation

To control the level of input synchronization, we generated patterns using the following procedure: (1) identical Poisson spike trains were first generated and assigned to all neurons

within a given pattern; (2) all spike events were then jittered independently across all stimulated neurons within a specified time window. By varying the width of this window, we systematically modulated the resulting input synchrony (Table 1), measured as Rsync (see Eq 2).

Input Rsync (mean ± sd)	**Temporal jitter window**
1.0 ± 0.0	0
0.55 ± 0.04	5
0.2 ± 0.06	20
0.1 ± 0.03	50

Table 1. Input synchrony

Temporal jitter window values used to generate patterns with specific levels of input Rsync, averaged over 100 trials for each jitter value.

References

Abeles, M. (1991). Corticonics: Neural circuits of the cerebral cortex. Cambridge University Press.

Anderson, B., Mruczek, R. E., Kawasaki, K., & Sheinberg, D. (2008). Effects of familiarity on neural activity in monkey inferior temporal lobe. *Cerebral cortex*, 18(11).

Baker, C. M., & Gong, Y. (2023). Identifying properties of pattern completion neurons in a computational model of the visual cortex. *PLoS Computational Biology*, 19(6), e1011167.

Brette, R. (2012). Computing with neural synchrony. *PLoS computational biology*, 8(6), e1002561.

Brette, R. (2015). Philosophy of the spike: rate-based vs. spike-based theories of the brain. Frontiers in systems neuroscience, 9.

Bosking, W. H., Zhang, Y., Schofield, B., & Fitzpatrick, D. (1997). Orientation selectivity and the arrangement of horizontal connections in tree shrew striate cortex. *Journal of neuroscience*, 17(6), 2112-2127.

Brown, M. W., Wilson, F. A. W., & Riches, I. P. (1987). Neuronal evidence that inferomedial temporal cortex is more important than hippocampus in certain processes underlying recognition memory. *Brain research*, 409(1).

Buzsaki, G., & Draguhn, A. (2004). Neuronal oscillations in cortical networks. *Science*, 304(5679), 1926-1929.

Carrillo-Reid, L., Han, S., Yang, W., Akrouh, A., & Yuste, R. (2019). Controlling visually guided behavior by holographic recalling of cortical ensembles. *Cell*, 178(2), 447-457.

Celebrini, S., Thorpe, S., Trotter, Y., & Imbert, M. (1993). Dynamics of orientation coding in area V1 of the awake primate. *Visual neuroscience*, 10(5), 811-825.

Chavane, F., Sharon, D., Jancke, D., Marre, O., Frégnac, Y., & Grinvald, A. (2011). Lateral spread of orientation selectivity in V1 is controlled by intracortical cooperativity. *Frontiers in systems neuroscience*, *5*, 4.

Clouter, A., Shapiro, K. L., & Hanslmayr, S. (2017). Theta phase synchronization is the glue that binds human associative memory. *Current Biology*, 27(20).

Cossell, L., Iacaruso, M. F., Muir, D. R., Houlton, R., Sader, E. N., Ko, H., ... & Mrsic-Flogel, T. D. (2015). Functional organization of excitatory synaptic strength in primary visual cortex. *Nature*, 518(7539), 399-403.

Derrington, A. (2001). The lateral geniculate nucleus. *Current Biology*, *11*(16), R635-R637.

Duke, D., Martin, C. B., Bowles, B., McRae, K., & Köhler, S. (2017). Perirhinal cortex tracks degree of recent as well as cumulative lifetime experience with object concepts. *Cortex*, *89*, 61-70.

Ermentrout, G. B., Galán, R. F., & Urban, N. N. (2008). Reliability, synchrony and noise. *Trends in neurosciences*, 31(8), 428-434.

Fecteau, J. H., & Munoz, D. P. (2006). Salience, relevance, and firing: a priority map for target selection. *Trends in cognitive sciences*, 10(8).

Frady, E. P., & Sommer, F. T. (2019). Robust computation with rhythmic spike patterns. *Proceedings of the National Academy of Sciences*, 116(36).

Fries, P., Roelfsema, P. R., Engel, A. K., König, P., & Singer, W. (1997). Synchronization of oscillatory responses in visual cortex correlates with perception in interocular rivalry. *Proceedings of the National Academy of Sciences*, 94(23).

Fries, P., Schröder, J. H., Roelfsema, P. R., Singer, W., & Engel, A. K. (2002). Oscillatory neuronal synchronization in primary visual cortex as a correlate of stimulus selection. *Journal of Neuroscience*, 22(9).

Galuske, R. A., & Singer, W. (1996). The origin and topography of long-range intrinsic projections in cat visual cortex: a developmental study. *Cerebral Cortex*, 6(3), 417-430.

Gollisch, T., & Meister, M. (2010). Eye smarter than scientists believed: neural computations in circuits of the retina. *Neuron*, 65(2), 150-164.

Hage, T. A., Bosma-Moody, A., Baker, C. A., Kratz, M. B., Campagnola, L., Jarsky, T., ... & Murphy, G. J. (2022). Synaptic connectivity to L2/3 of primary visual cortex measured by two-photon optogenetic stimulation. *elife*, 11, e71103.

Hayden, D. J., Finnie, P. S., Thomazeau, A., Li, A. Y., Cooke, S. F., & Bear, M. F. (2023). Electrophysiological signatures of visual recognition memory across all layers of mouse V1. *Journal of Neuroscience*, 43(44).

Hopfield, J. J. (1982). Neural networks and physical systems with emergent collective computational abilities. *Proceedings of the national academy of sciences*, 79(8), 2554-2558.

Hu, D., Sato, T., Rockland, K. S., Tanifuji, M., & Tanigawa, H. (2025). Relationship between functional structures and horizontal connections in macaque inferior temporal cortex. *Scientific Reports*, *15*(1), 3436.

Huang, X., Elyada, Y. M., Bosking, W. H., Walker, T., & Fitzpatrick, D. (2014). Optogenetic assessment of horizontal interactions in primary visual cortex. *Journal of Neuroscience*, *34*(14), 4976-4990.

Kazanovich, Y., & Borisyuk, R. (2021). A computational model of familiarity detection for natural pictures, abstract images, and random patterns: Combination of deep learning and anti-Hebbian training. *Neural Networks*, *143*, 628-637.

Koolschijn, R. S., Emir, U. E., Pantelides, A. C., Nili, H., Behrens, T. E., & Barron, H. C. (2019). The hippocampus and neocortical inhibitory engrams protect against memory interference. *Neuron*, 101(3).

Korndörfer, C., Ullner, E., García-Ojalvo, J., & Pipa, G. (2017). Cortical spike synchrony as a measure of input familiarity. *Neural computation*, 29(9).

Lee, W. C. A., Bonin, V., Reed, M., Graham, B. J., Hood, G., Glattfelder, K., & Reid, R. C. (2016). Anatomy and function of an excitatory network in the visual cortex. *Nature*, *532*(7599), 370-374.

Levitt, J. B., Yoshioka, T., & Lund, J. S. (1994). Intrinsic cortical connections in macaque visual area V2: evidence for interaction between different functional streams. *Journal of Comparative Neurology*, *342*(4), 551-570.

Litwin-Kumar, A., & Doiron, B. (2014). Formation and maintenance of neuronal assemblies through synaptic plasticity. *Nature communications*, *5*(1), 5319.

Lovett-Barron, M., Kaifosh, P., Kheirbek, M. A., Danielson, N., Zaremba, J. D., Reardon, T. R., ... & Losonczy, A. (2014). Dendritic inhibition in the hippocampus supports fear learning. *Science*, 343(6173).

Mainen, Z. F., & Sejnowski, T. J. (1995). Reliability of spike timing in neocortical neurons. *Science*, 268(5216), 1503-1506.

Malach, R., Tootell, R. B., & Malonek, D. (1994). Relationship between orientation domains, cytochrome oxidase stripes, and intrinsic horizontal connections in squirrel monkey area V2. *Cerebral Cortex*, *4*(2), 151-165.

Nakazawa, K., Quirk, M. C., Chitwood, R. A., Watanabe, M., Yeckel, M. F., Sun, L. D., ... & Tonegawa, S. (2002). Requirement for hippocampal CA3 NMDA receptors in associative memory recall. *Science*, 297(5579), 211-218.

Naud, R., & Sprekeler, H. (2018). Sparse bursts optimize information transmission in a multiplexed neural code. *Proceedings of the National Academy of Sciences*, 115(27), E6329-E6338.

Niell, C. M., & Stryker, M. P. (2008). Highly selective receptive fields in mouse visual cortex. *Journal of Neuroscience*, 28(30).

Norman, K. A., & O'Reilly, R. C. (2003). Modeling hippocampal and neocortical contributions to recognition memory: a complementary-learning-systems approach. *Psychological review*, *110*(4), 611.

Onat, S., König, P., & Jancke, D. (2011). Natural scene evoked population dynamics across cat primary visual cortex captured with voltage-sensitive dye imaging. *Cerebral cortex*, 21(11).

Palva, J. M., Palva, S., & Kaila, K. (2005). Phase synchrony among neuronal oscillations in the human cortex. *Journal of Neuroscience*, 25(15).

Panzeri, S., Ince, R. A., Diamond, M. E., & Kayser, C. (2014). Reading spike timing without a clock: intrinsic decoding of spike trains. *Philosophical Transactions of the Royal Society B: Biological Sciences*, 369(1637), 20120467.

Rainer, G., & Miller, E. K. (2000). Effects of visual experience on the representation of objects in the prefrontal cortex. *Neuron*, 27(1).

Rathbun, D. L., Alitto, H. J., Warland, D. K., & Usrey, W. M. (2016). Stimulus contrast and retinogeniculate signal processing. *Frontiers in neural circuits*, 10, 8.

Roelfsema, P. R., Engel, A. K., König, P., & Singer, W. (1996). The role of neuronal synchronization in response selection: A biologically plausible theory of structured representations in the visual cortex. *Journal of Cognitive Neuroscience*, 8(6).

Sanchez, A. N., Alitto, H. J., Rathbun, D. L., Fisher, T. G., & Usrey, W. M. (2023). Stimulus contrast modulates burst activity in the lateral geniculate nucleus. *Current Research in Neurobiology*, 4.

Scarpetta, S., & Giacco, F. (2013). Associative memory of phase-coded spatiotemporal patterns in leaky Integrate and Fire networks. *Journal of Computational Neuroscience*, 34.

Schmidt, K. E., Galuske, R. A., & Singer, W. (1999). Matching the modules: Cortical maps and long-range intrinsic connections in visual cortex during development. *Journal of neurobiology*, 41(1), 10-17.

Shadlen, M. N., & Movshon, J. A. (1999). Synchrony unbound: a critical evaluation of the temporal binding hypothesis. *Neuron*, 24(1).

Sigman, M., Cecchi, G. A., Gilbert, C. D., & Magnasco, M. O. (2001). On a common circle: natural scenes and Gestalt rules. *Proceedings of the National Academy of Sciences*, 98(4).

Singer, W. (1999). Neuronal synchrony: a versatile code for the definition of relations? *Neuron*, 24(1).

Softky, W. R., & Koch, C. (1993). The highly irregular firing of cortical cells is inconsistent with temporal integration of random EPSPs. *Journal of neuroscience*, 13(1).

Sweeney-Reed, C. M., Zaehle, T., Voges, J., Schmitt, F. C., Buentjen, L., Kopitzki, K., ... & Richardson-Klavehn, A. (2014). Corticothalamic phase synchrony and cross-frequency coupling predict human memory formation. *elife*, 3, e05352.

Szatmáry, B., & Izhikevich, E. M. (2010). Spike-timing theory of working memory. PLoS computational biology, 6(8), e1000879.

Taylor, L., Zenke, F., King, A. J., & Harper, N. S. (2024). Temporal prediction captures key differences between spiking excitatory and inhibitory V1 neurons. *bioRxiv*, 2024-05.

Thorpe, S., Delorme, A., & Van Rullen, R. (2001). Spike-based strategies for rapid processing. *Neural networks*, 14(6-7).

Tsunoda, K., Yamane, Y., Nishizaki, M., & Tanifuji, M. (2001). Complex objects are represented in macaque inferotemporal cortex by the combination of feature columns. *Nature neuroscience*, *4*(8), 832-838.

Ts'o, D. Y., Gilbert, C. D., & Wiesel, T. N. (1986). Relationships between horizontal interactions and functional architecture in cat striate cortex as revealed by cross-correlation analysis. *Journal of neuroscience*, 6(4).

Tyulmankov, D., Yang, G. R., & Abbott, L. F. (2022). Meta-learning synaptic plasticity and memory addressing for continual familiarity detection. *Neuron*, 110(3), 544-557.

Xie, W., Wittig Jr, J. H., Chapeton, J. I., El-Kalliny, M., Jackson, S. N., Inati, S. K., & Zaghloul, K. A. (2024). Neuronal sequences in population bursts encode information in human cortex. *Nature*, 1-8.

Yang, H., McRae, K., & Köhler, S. (2023). Perirhinal cortex automatically tracks multiple types of familiarity regardless of task-relevance. *Neuropsychologia*, *187*, 108600.

Zemliak, V., Mayer, J., Nieters, P., & Pipa, G. (2024). Spike synchrony as a measure of Gestalt structure. *Scientific Reports*, 14(1).

Zemliak, V., Pipa, G., & Nieters, P. (2025). Continual familiarity decoding from recurrent connections in spiking networks. *bioRxiv*, 2025-01.

Znamenskiy, P., Kim, M., Muir, D. R., Iacaruso, M. F., Hofer, S. B., & Mrsic-Flogel, T. D. (2018). Functional selectivity and specific connectivity of inhibitory neurons in primary visual cortex. *bioRxiv* 294835.